Melting of colloidal crystals: A Monte Carlo study

James C. Zahorchak, R. Kesavamoorthy,[a),b)] Rob D. Coalson, and Sanford A. Asher[b)]
Materials Research Center and Department of Chemistry, University of Pittsburgh, Pittsburgh, Pennsylvania 15260

(Received 31 October 1991; accepted 23 January 1992)

Electrostatically stabilized colloidal crystals show phase transitions into liquid and gaslike states as the ionic impurity concentration increases. Using Monte Carlo simulations we theoretically investigate the melting of four colloidal crystals (two fcc crystals and two bcc crystals) which have also been examined experimentally. We calculate the pair correlation function $g(r)$, the total potential energy U_t, and the mean square displacement of a particle $\langle u^2 \rangle$ for the colloidal suspensions at various ionic impurity concentrations n_i. We calculate the structure factor $S(Q)$ by Fourier transforming $g(r)$. We find that the parameters $g_{\max}$ [the maximum of the first peak in $g(r)$], $S_{\max}$ [the maximum of the first peak in $S(Q)$], Δr [the half width at half maximum of the first peak in $g(r)$], and U_t (the total potential energy) all show discontinuous behavior on melting. We relate the calculated values of $S_{\max}$, $g_{\max}$, and the mean square displacement at the point of melting of our colloidal crystals to that of atomic crystals. We find that the ratio of the rate of change of the Wendt–Abraham parameter, $g_{\min}/g_{\max}$ [$g_{\min}$: the minimum value of $g(r)$ after the first peak], with respect to n_i, in colloidal crystal to that in liquid is constant but specific to the crystal structure (bcc or fcc). We calculate the latent heat of melting of colloidal crystals.

I. INTRODUCTION

Since colloid ordering occurs at easily studied macroscopic length scales,[1–7] suspensions of monodisperse colloidal spheres are frequently used as model systems to study phases and phase transitions. Aqueous suspensions of charged colloidal spheres show gas, liquid, glass, and crystalline phases on length scales of nanometers to microns.[1,3,8–11] These phases form spontaneously and the stable phase depends on parameters such as the ionic impurity concentration (n_i), particle concentration (n_p), particle charge (Ze), particle diameter (σ), temperature (T), and the solvent dielectric constant (ϵ).[1,8–12]

Each particle is surrounded by a diffuse ion cloud extending from the particle surface into the solution. The interparticle interaction is well represented by a screened Coulomb repulsive potential extending over several particle diameters. The formation of a cubic crystalline structure minimizes these repulsive interactions; the lattice parameter is completely determined by the particle concentration and crystal structure. Highly efficient colloid crystal optical filters, which Bragg diffract to reject narrow bandwidths of light, have been developed and are commercially available.[13,14]

Colloidal crystals are known to exist in body centered cubic (bcc) and face centered cubic (fcc) structures depending on Z, n_p, and σ.[2,3,9,15] Suspensions of particles of diameter of ca. 100 nm and particle charge numbers 600, form bcc structures for $n_p < 3 \times 10^{13}$ cm^{-3} and form fcc structures at higher n_p.[3,15] When the particle effective charge[8] is increased to 1150, the crystal remains in bcc for $n_p \sim 1 \times 10^{14}$ cm^{-3}. However, at higher n_p values the structure is fcc.[16] For larger particle diameters (~ 500 nm) colloidal crystals show fcc structure even at $n_p = 10^{11}$ cm^{-3}.[17–19]

Colloidal crystals can be melted by increasing n_i,[4,7,12] increasing T[6,11,20] or reducing n_p. Various phases and phase transitions have been theoretically predicted in colloidal suspension by utilizing free energy calculations,[2,10] density functional formulations,[21,22] and computer simulations.[1,9]

Crystal to liquid phase transitions in atomic crystals are characterized by the Lindemann criteria,[23] which states that a crystal will melt when the root mean square displacement of the atoms from their equilibrium positions, $\langle u^2 \rangle^{1/2}$, becomes about 10% of $n_p^{-1/3}$, the average interparticle distance. However, previous predictions indicate that colloidal crystals melt when $\langle u^2 \rangle^{1/2}$ reaches about 19% of $n_p^{-1/3}$.[2,9,24] Ise *et al.*[17] have observed the dynamics of a single colloidal particle in a crystal using an optical microscope and image processor, and have demonstrated that crystalline phases exist with $\langle u^2 \rangle^{1/2} \cong 0.16 n_p^{-1/3}$.

Kesavamoorthy *et al.*[4] utilized static light scattering to study the freezing of colloid liquids and found $S_{\max}$ [the maximum of the first peak in the structure factor, $S(Q)$] for colloidal bcc crystals to be 2.1 at freezing. In constrast, $S_{\max}$ in atomic systems is 2.8 for fcc crystals and 3.1 for bcc crystals.[25–28] In an effort to understand the universal value of $S_{\max}$ at freezing of atomic liquids, Verlet[29] studied hard spheres systems utilizing the Kirkwood–Alder freezing criterion[30] (which states that the volume fraction of hard spheres at freezing is 0.49). They calculated $S_{\max} = 2.85$ from computer simulations. Ramakrishnan and Yussouff[21] developed a density functional theory for the freezing of atomic liquids which was consistent with both computer simulation[30,31] and experiments.[25–28]

a) Materials Science Division, Indira Gandhi Centre for Atomic Research, Kalpakkam 603102, India.
b) Authors to whom correspondence should be addressed.

 0021-9606/92/096873-07$06.00

The Wendt–Abraham parameter,[32] R_g [$R_g = g_{\min}/g_{\max}$, where $g_{\min}$ is the minimum value of $g(r)$ following the first peak and $g_{\max}$ is the maximum value of $g(r)$], is useful for studying phase transitions.[32] Kimura and Yonezawa have investigated the liquid to glass transition of argon using computer simulated quenching of liquid argon at different temperatures. They found that R_g was continuous, but a change in the temperature derivative of R_g occured at the glass transition temperature;[33] R_g is expected to be continuous at the liquid-glass transition, but not at the liquid-crystal transition.

In the present work we use Metropolis Monte Carlo (MC) sampling[34,35] to simulate aqueous charged monodisperse colloidal suspensions containing various ionic impurity concentrations. We examine the melting of fcc and bcc crystals by increasing the ionic impurity concentration at constant T, volume, and n_p. We obtain the pair correlation function, $g(r)$, the total potential energy U_t, and the mean square displacement $\langle u^2 \rangle$. The structure factor is obtained by Fourier transforming $g(r)$. We find similar values for these structural parameters for different bcc crystals. However, these bcc values differ from those of fcc crystals. The Lindemann criterion is found to be the same for both bcc and fcc colloidal crystals. We also calculate the latent heat of melting of these crystals.

II. SIMULATION DETAILS

Monte Carlo simulations based on Metropolis algorithm[34,35] for a canonical ensemble (constant number of particles, volume, and temperature) were carried out with periodic boundary conditions to simulate aqueous colloidal suspensions of monodisperse polystyrene particles. The particles interact via a screened Coulomb potential[7]

$$U(r) = \frac{Z^2 e^2}{\epsilon}\left[\frac{\exp(\kappa\sigma/2)}{1+\kappa\sigma/2}\right]^2 \frac{\exp(-\kappa r)}{r}, \tag{1}$$

where Ze is the charge on the particles of diameter σ, e is the electronic charge, ϵ is the static dielectric constant of the medium, and r is the interparticle separation distance. The inverse Debye screening length, κ, is given by

$$\kappa^2 = \frac{4\pi e^2}{\epsilon k_B T}[n_p Z + n_i], \tag{2}$$

where k_B is Boltzmann constant, n_p is the particle concentration, n_i is the ionic impurity concentration (assumed to be monovalent), and $n_p Z$ is the counter ion concentration. When the suspension is really pure ($n_i = 0$), then the particle screening ions are only the counter ions with concentration $n_p Z$. If the water is impure or a typical 1:1 ionic salt is added to the suspension, the particle screening ion concentration becomes $n_p Z + n_i$, where n_i is the added impurity concentration (positive + negative ions). In experiments, n_i represents the impurity concentration originally present in water and that added intentionally to the suspension.[7] All simulations are performed at $T = 298$ K. Table I lists the parameters for the for colloidal systems simulated, which are similar to systems that have been previously studied experimentally.[4,16,36,37] Systems A and B prepared from polystyrene spheres exist in bcc structure while systems C and D exist in fcc structure. Each simulation begins by loading 250 particles in bcc lattice positions for systems A and B or by loading 256 particles in fcc lattice positions for systems C and D in a cubic cell of volume $V = L^3 = N/n_p$. MC simulations with $N = 250$ are known to give similar results to those using $N \geqslant 500$.[21,38] The potential energy calculations are cut off at $r = L/2$, because at this distance the interaction pair potential is less than $10^{-4} k_B T$. This cutoff is comparable to that used previously.[38,39] Step sizes of $\sigma/2$ were chosen for systems A, B, and C and $\sigma/4$ for system D. The total potential energy is calculated after each particle is moved a step in a random direction. The new configuration is accepted or rejected via Boltzmann weighted energy comparisons. One MC pass occurs when all N particles have moved once. Approximately 4000 passes (~ 1.1 million configurations) are discarded initially while the system evolves to equilibrium.[22,38] After reaching equilibrium, the pair correlation function, mean square displacement of all particles, and the total potential energy are obtained by calculating 350 more passes. The total potential energy is found to fluctuate negligibly about a mean value which is constant for the final 350 passes, confirming that the system has equilibrated.

TABLE I. The details of the colloidal systems simulated.

System	$n_p/10^{13}$ cm^{-3}	σ/nm	Z	Crystal structure	Ref.
A	0.42	109	600	bcc	4
B	8	83	1150	bcc	16
C	8	83	600	fcc	36
D	16	83	1150	fcc	37

The pair correlation function $g(r)$ is obtained for $r = 0$ to $L/2$ using the standard methods.[39] The total potential energy is obtained from[32,36,38,39]

$$U_t = \frac{1}{2}\sum_{j\neq i}^{N}\sum_{i=1}^{N} U(r_{ij}). \tag{3}$$

An approximate value of the mean square displacement $\langle u^2 \rangle$, is obtained from Δr, the half width at half maximum of the first peak in $g(r)$. The width of the first peak in $g(r)$ is related to the average displacement of the first nearest neighbor particles from their equilibrium position. Hone *et al.*[2] point out that thermal averaging of the colloidal particle density function relates the bandwidth of the first peak in $g(r)$ to $\langle u^2 \rangle$,

$$g_1(r) = (g_{\max})\exp\left[-\frac{3(r-d)^2}{2\langle u^2\rangle}\right], \tag{4}$$

where d is the average interparticle separation distance. Thus, from Eq. (4),

$$\langle u^2 \rangle = \frac{3(\Delta r)^2}{2\ln(2)}. \tag{5}$$

Equation (5) can be used to determine $\langle u^2 \rangle$ in the crystal phase where the particles vibrate around their equilibrium position. In constrast, Eq. (5) might not be helpful to obtain

$\langle u^2 \rangle$ in liquid phase where the particles undergo diffusive motion. However, in order to compute the Lindemann melting parameter, W, it is sufficient to calculate $\langle u^2 \rangle$ in crystal phase using Eq. (5). We may also determine the mean square displacement (MSD) of a particle from the variation in position between different passes (m),

$$\mathrm{MSD}(m) = \frac{1}{N} \sum_{i=1}^{N} (r_{i,m} - r_{i,4000})^2, \tag{6}$$

where $r_{i,4000}$ is the position of the ith particle at pass number 4000. MSD(m) was calculated for m ranging from 4000 to 4350. We compare these two methods for calculating the mean square displacment in Sec. III D.

Each simulation is initiated from a system with perfect crystalline order. As the simulation proceeds, the system relaxes into either a less rigid crystalline state or melts into a liquid state depending upon the ionic impurity concentration. The simulations were performed on the FPS model 500EA computer and the CPU time required for each simulation was ~4.5 hours.

The static structure factor, $S(Q)$ is obtained by Fourier transforming $g(r)$,

$$S(Q) = 1 + \frac{4\pi n_p}{Q} \int_{r=0}^{L/2} [g(r) - 1] \sin(Qr) dr. \tag{7}$$

Since $g(r)$ was calculated from $r = 0$ to $L/2$, the integration in Eq. (7) was truncated at $L/2$. Becuase of this truncation, $S(Q)$ oscillates with considerable amplitude at small values of Q [i.e., $Q = 0$ to $0.7(2\pi/d)$ where d is the average interparticle separation]. Thus, for this range of Q, $S(Q)$ was assigned a value of zero. $S(Q)$ was calculated for $Q = 0.7(2\pi/d)$ to $3.5(2\pi/d)$. Each $g(r)$ obtained by an inverse transform of the calculated $S(Q)$ was identical to the original $g(r)$ to within ± 0.05.

III. RESULTS AND DISCUSSION

The dependence of all of the structural parameters, $g_{\max}$, R_g, $S_{\max}$ on ionic impurity concentration, for each crystal, are similar: thus the values of each parameter can be used to develop melting criteria. We discuss each parameter individually since all have been used in different previous melting investigations.[4,20,33]

A. $g_{\max}$

Figure 1, which shows the plots of $g_{\max}$ (the maximum value of the first peak) as a function of n_i for the colloidal crystals, indicates that $g_{\max}$ decreases monotonically as n_i increases. For each of these colloids, $g_{\max}$ discontinuously decreases at a particular critical ionic impurity concentration, n_i^m. The rate of decrease of $g_{\max}$ with n_i is larger in the region $n_i < n_i^m$ than in the region $n_i > n_i^m$.

Figure 2 shows two calculated $g(r)$ curves for the fcc colloid system C. The solid plot shows a $g(r)$ for $n_i < n_i^m$, while the dashed plot shows a $g(r)$ for $n_i > n_i^m$. For $n_i < n_i^m$, $g(r)$ of Fig. 2 shows peaks at r values of various neighbor positions associated with a crystalline order. In contrast, for $n_i > n_i^m$, $g(r)$ shows smoother peaks which more quickly decrease in magnitude at higher r. This behavior is characteristic of liquid order. It appears that the colloidal crystal melts at n_i^m since the observed discontinuity in $g_{\max}$ at n_i^m is characteristic of a first order phase transition.[40] Table II lists the $g_{\max}$ values at n_i^m in both crystal ($g_{\max}^c$) and liquid ($g_{\max}^l$) phases and illustrates that n_i^m for melting is different for each crystal. $g_{\max}^c$ are essentially the same at 2.85 ± 0.05 for both bcc crystals, but are smaller (2.72 ± 0.05) for the fcc crystals. Similarly, $g_{\max}^l$ are the same for the two bcc crystals at 2.61 ± 0.05, but are smaller (2.48 ± 0.05) for fcc crystals.

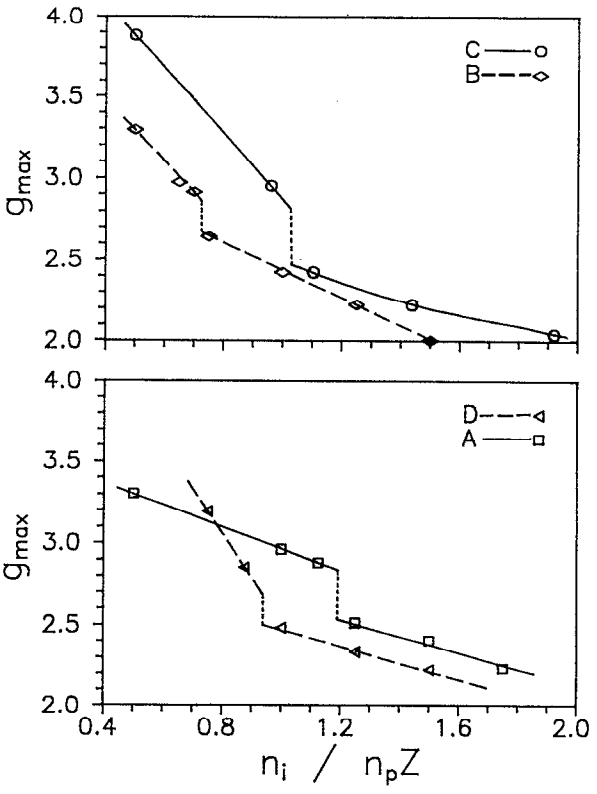

FIG. 1. Maximum height of the first peak of the pair correlation function $g_{\max}$ as a function of n_i for colloid systems A to D.

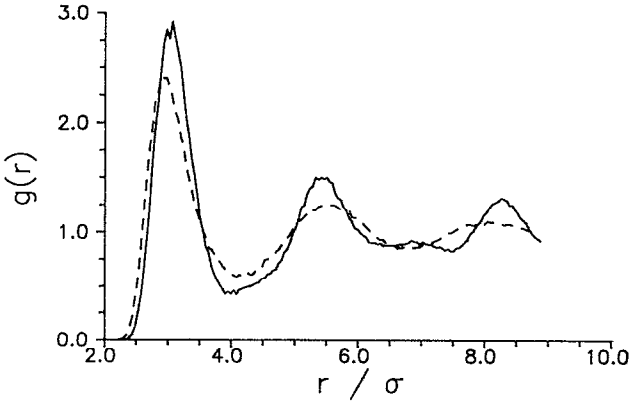

FIG. 2. Pair correlation functions $g(r)$ for colloid system C. (—) fcc crystalline structure for $n_i/n_pZ = 0.958$, (- - - - - -) liquid structure for $n_i/n_pZ = 1.104$.

TABLE II. The simulation results on the structural parameters of the colloidal suspensions.

System	*A*	*B*	*C*	*D*
n_i^m/n_p^Z	1.19 ± 0.06	0.72 ± 0.03	1.03 ± 0.07	0.94 ± 0.06
$g_{\max}^c$	2.85 ± 0.05	2.84 ± 0.05	2.77 ± 0.05	2.68 ± 0.05
$g_{\max}^l$	2.57 ± 0.05	2.66 ± 0.05	2.47 ± 0.05	2.50 ± 0.05
m_g	0.78 ± 0.03	0.74 ± 0.03	0.61 ± 0.03	0.62 ± 0.03
$S_{\max}^c$	3.30 ± 0.07	3.19 ± 0.07	2.82 ± 0.07	2.70 ± 0.07
$S_{\max}^l$	2.49 ± 0.05	2.54 ± 0.05	2.38 ± 0.05	2.41 ± 0.05

These are the first reports, to our knowledge, of the values of $g_{\max}$ at melting for colloidal crystals.

B. R_g

Figure 3 shows the Wendt–Abraham parameter, $R_g = g_{\min}/g_{\max}$. R_g is probably more sensitive to melting than $g(r)$ since the ratio will be independent of the scaling of $g(r)$. R_g as a function of n_i also shows a discontinuity at n_i^m. The slope of R_g is lower in the liquid state than in the corresponding crystalline state; Table II lists the ratio of these slopes, m_g. m_g is essentially identical for both bcc crystals (0.76 ± 0.03), but is smaller (0.61 ± 0.03) for the fcc crystals. The Wendt–Abraham parameter, which was previously used to theoretically investigate the glass to liquid transition of argon,[33] was found to be continuous across the glass to

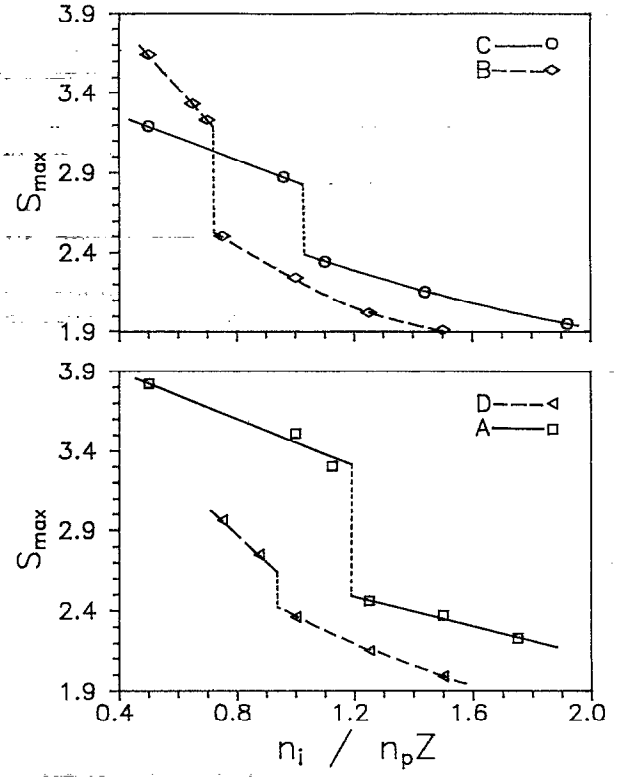

FIG. 4. Maximum height of the first peak of the structure factor $S_{\max}$ as a function of n_i for systems *A* to *D*.

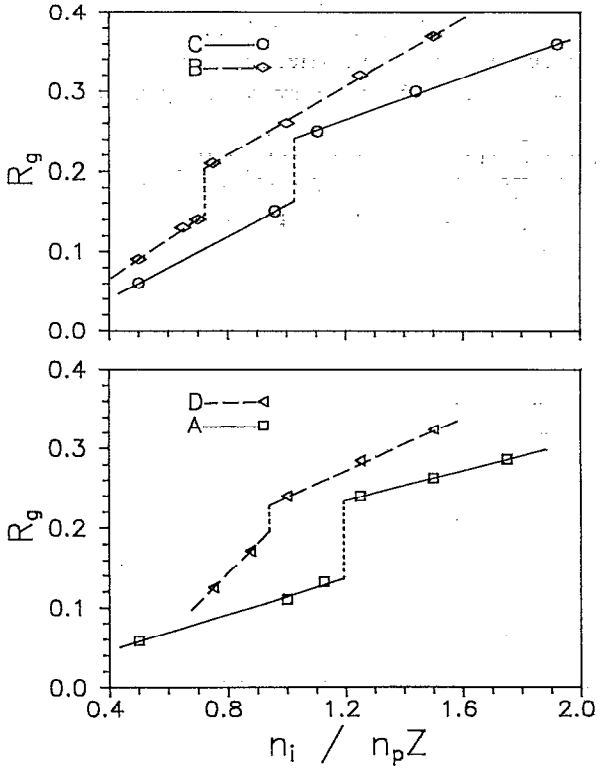

FIG. 3. The Wendt–Abraham parameter R_g as a function of n_i for systems *A* to *D*.

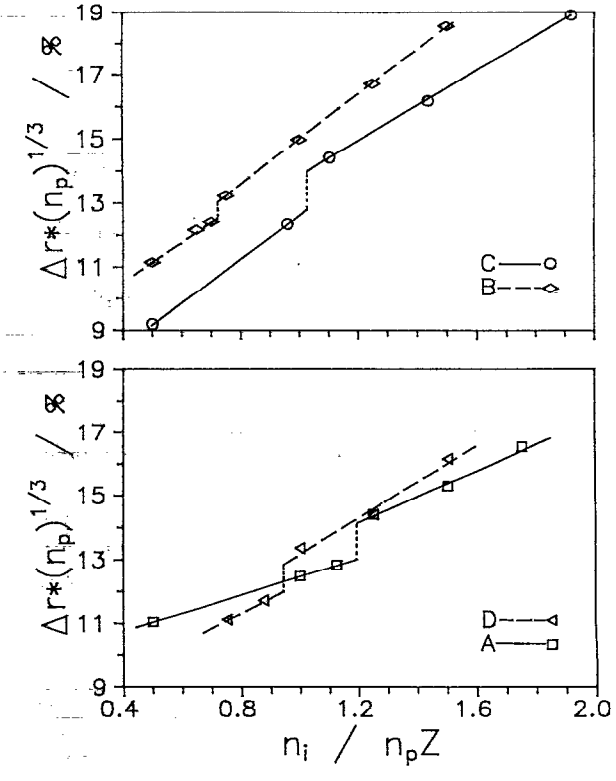

FIG. 5. Half width at half maximum height of the first peak of the pair correlation function Δr as a function of n_i for systems *A* to *D*.

TABLE III. Simulation results on the mean square displacement and the energy of the colloidal suspensions.

System	*A*	*B*	*C*	*D*
$\Delta r * n_p^{1/3}$	0.130 ± 0.005	0.126 ± 0.005	0.128 ± 0.005	0.121 ± 0.005
W	0.191 ± 0.005	0.185 ± 0.005	0.188 ± 0.005	0.178 ± 0.005
$\mathrm{RMSD} * n_p^{1/3}$	0.27 ± 0.01	0.32 ± 0.01	0.31 ± 0.01	0.36 ± 0.01
$\Delta U/10^{-12}$ erg	5.6 ± 0.3	5.5 ± 0.3	5.7 ± 0.3	4.7 ± 0.3
$\Delta S/10^{-14} \frac{\text{erg}}{K}$	1.9 ± 0.1	1.9 ± 0.1	1.9 ± 0.1	1.6 ± 0.1
$L/\frac{\text{cal}}{\text{mol}}$	320 ± 20	320 ± 20	320 ± 20	270 ± 20

liquid transition (which is not a first order transition), but showed a discontinuity in slope at the transition point. In the present work R_g is discontinuous across the melting transition, a finding consistent with a first order phase transition.

C. S_{max}

Figure 4 shows the dependence of S_{max} on n_i: S_{max} is obtained from the Fourier transform of $g(r)$. As observed for g_{max} and R_g, S_{max} also shows a discontinuity at n_i^m. The value of S_{max} at n_i^m in the crystalline state, S_{max}^c, is 3.25 ± 0.07 for both bcc crystals, but decreases to 2.76 ± 0.07 for the fcc crystals. The corresponding S_{max} values in the liquid state, S_{max}^l, are 2.52 ± 0.05 for the bcc crystals and 2.39 ± 0.05 for the fcc crystals. Table II lists these S_{max} values. Consistent with our observations, liquid metals which freeze into bcc structure give larger $S_{max}^l = 3.1$ values than those that freeze into fcc structure, $S_{max}^l = 2.8$.[25–28]

Kesavamoorthy *et al.*[4] have experimentally measured a value of $S_{max}^l = 2.1 \pm 0.1$ for system *A*, which significantly differs from the present simulation value of $S_{max}^l = 2.52 \pm 0.05$. The origin of this discrepancy is not clear at present. However, Kesavamoorthy *et al.*[4] kept a mixed bed of ion-exchange resins at the bottom of the suspension, which caused a gradient in n_i along the height of the column. The upper region of the suspension was liquid while the bottom region was crystalline. Because of the n_i gradient, n_i in the measurement region (about 1–2 mm above the liquid-crystal boundary) could have been higher than n_i^m which would result in a lowered S_{max}^l value. Also, the experiment was carried out under constant pressure conditions while the simulation is performed under constant volume conditions.

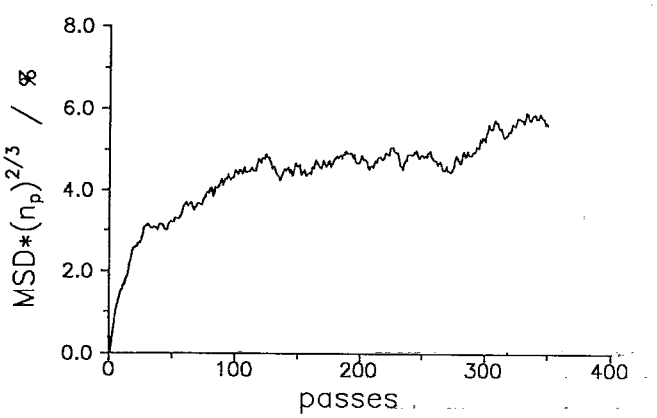

FIG. 6. Mean square displacement (MSD) as a function of the number of Monte Carlo passes for colloid system *B*, in crystalline phase, at $n_i/n_pZ = 0.500$.

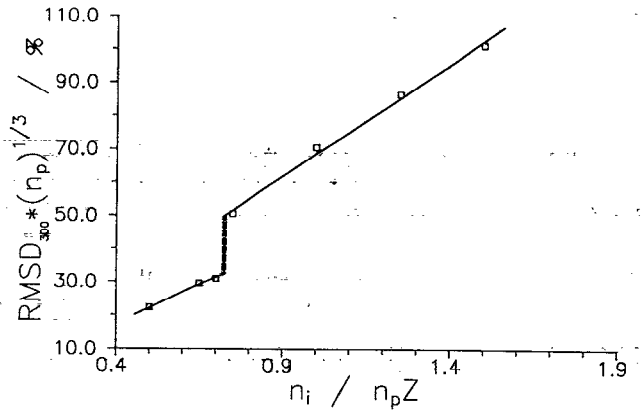

FIG. 7. Root mean square displacement (RMSD) (at the 300th pass) as a function of n_i for system *B*.

D. Mean square displacement

The mean square displacement, $\langle u^2 \rangle$, is obtained from Δr from the first peak of the $g(r)$ using Eq. (5). Figure 5 shows Δr as a function of n_i, while Table III lists the values of Δr_m (where the crystal just begins to melt) as well as the

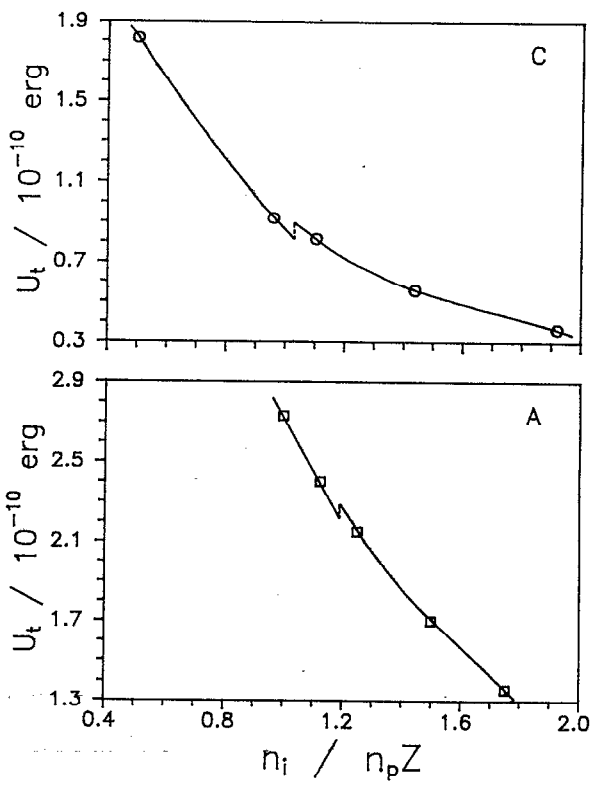

FIG. 8. Total equilibrium potential energy U_t as a function of n_i for systems *A* and *C*.

Lindemann parameter, $W = n_p^{1/3}[\langle u^2 \rangle]^{1/2}$. W at n_i^m is the same for the bcc and fcc crystals ($W = 0.19 \pm 0.01$) to within our calculated accuracy and is identical to values of W obtained by others.[1,2,7,9,24]

Tata *et al.*[41] have obtained the mean square displacement (MSD) of a particle at equilibrium. They calculated the root mean square displacement (RMSD) to be 28% of $n_p^{1/3}$ at n_i^m.[41] Figure 6 shows a typical MSD plot as a function of m for the bcc colloidal crystal B. Figure 7 shows MSD as a function of n_i for the system B after 300 passes, while Table III lists RMSD at n_i^m for each system. Our calculated RMSD is significantly larger than $[\langle u^2 \rangle]^{1/2}$ because it includes deviation in position relative to the original lattice site and does not permit the lattice to move as the crystal relaxes. Moreover, MSD depends on the number of passes (m). Even for a large value of $m(>300)$, MSD increases with m. The high values of RMSD$^* n_p^{1/3}$ at melting observed by Tata *et al.*[41] and us (the present work) as compared to W clearly indicates that it is incorrect to determine W on the basis of the calculated MSD value of Eq. (6).

E. Total potential energy

Figures 8 and 9 which show the total potential energy, U_t [calculated using Eq. (3)], as a function of n_i, indicates that U_t decreases monotonically with n_i in both the crystalline and in the liquid phases. U_t discontinuously increases by a value ΔU at n_i^m. This ΔU increase (for N particles), derives from the change in entropy at 298 K. The change in Helmholtz free energy, ΔF, should be zero at n_i^m:[40]

$$\Delta F = 0 = \Delta U = T\Delta S, \tag{8}$$

where ΔS is the entropy increase on melting. The values of ΔU and ΔS [obtained using Eq. (7)] are listed in Table III. The latent heat of melting, L, can be obtained from ΔU; Table III shows that L is essentially identical, ~ 320 cal/mole for all the colloidal crystals. Previously Williams *et al.* experimentally melted colloidal crystals increasing T and calculated the latent heat of melting using an approximate theory.[11] Their value of L (~ 4 kcal/mole) is dramatically different from ours. In our study, the colloidal crystals melt due to an increase in n_i at constant temperature and volume.

We simulated the melting of system A with $n_i = 1.15 n_p Z$ by increasing the temperature. Our preliminary results indicate that system A melts at ~ 360 K with a latent heat of melting, $L \sim 630$ cal/mole. In this simulation, we account for the temperature dependence of ϵ but ignore the thermal expansion of the suspension. MC simulation at constant pressure would be more appropriate for a system which is expanding due to increasing temperature.

A real experimental determination of L is fraught with aritfacts. Increasing T causes an increase in the ionic impurity concentration due to leaching from the container walls. In addition, convection currents will occur to cause shear induced melting.

IV. CONCLUSION

We have used Monte Carlo simulation techniques to study the melting of electrostatically stabilized colloidal particles. Two bcc and two fcc colloidal crystals were melted by increasing the ionic impurity concentration at constant temperature and volume. All structural parameters, g_{max}, S_{max}, and R_g show values at melting which differ between the bcc crystals and fcc crystals. We establish melting criteria based on these structural parameter values at melting and compare these criteria to those in atomic systems. The Lindemann criterion which is obtained from the width of the simulated $g(r)$ first peak compares well with other reported values. We estimate the latent heat of melting and the entropy increase at melting from the potential energy increase.

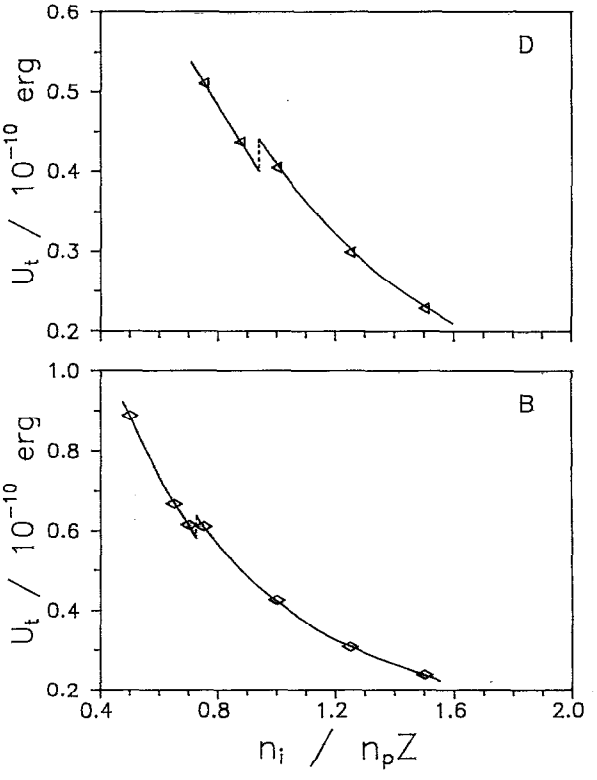

FIG. 9. Total equilibrium potential energy U_t as a function of n_i for systems B and D.

ACKNOWLEDGMENTS

We gratefully acknowledge support by the University of Pittsburgh Materials Research Center. J. C. Z. and R. D. C. acknowledge partial financial support of the National Science Foundation Grant No. CHE-9101432 and computational support of the Pittsburgh Supercomputer Center. Many of the calculations were carried out on the University of Pittsburgh Chemistry Department's FPS Model 500EA computer which was funded by the National Science Foundation.

[1] D. Thirumalai, J. Phys. Chem. **93**, 5673 (1989).
[2] D. Hone, S. Alexander, P. M. Chaikin, and P. Pincus, J. Chem. Phys. **79**, 1474 (1983).
[3] H. M. Lindsay and P. M. Chaikin, J. Chem. Phys. **76**, 3774 (1982).
[4] R. Kesavamoorthy, B. V. R. Tata, A. K. Arora, and A. K. Sood, Phys. Lett. A **138**, 208 (1989).
[5] W. Y. Shih, I. A. Aksay, and R. Kikuchi, J. Chem. Phys. **86**, 5127 (1987).
[6] D. W. Schaefer, J. Chem. Phys. **66**, 3980 (1977).

[7]A. K. Sood, in *Solid State Physics 45*, edited by H. Ehrenreich and D. Turnbull (Academic, New York, 1991).
[8]Y. Monovoukas and A. P. Gast, J. Colloid Interface Sci. **128**, 533 (1989).
[9]M. O. Robbins, K. Kremer, and G. S. Grest, J. Chem. Phys. **88**, 3286 (1988).
[10]W. Shih and D. Stroud, J. Chem. Phys. **79**, 6254 (1983).
[11]R. Williams, R. S. Crandell, and P. J. Wojtowicz, Phys. Rev. Lett. **37**, 348 (1976).
[12]W. B. Russel, D. A. Saville, and W. R. Schowalter, *Colloidal Dispersions* (Cambridge University, New York, 1989).
[13]S. A. Asher, P. L. Flaugh, and G. Washinger, Spectroscopy **1**, 26 (1986).
[14]S. A. Asher, U. S. Patent Nos. 4,627,689 and 4,632,517.
[15]M. K. Udo and M. F. de Souza, Solid State Commun. **35**, 907 (1980).
[16]P. A. Rudquist, R. Kesavamoorthy, S. Jagannathan, and S. A. Asher, J. Chem. Phys. **95**, 1249 (1991).
[17]N. Ise, Angew. Chem. Int. Ed. Engl. **25**, 323 (1986).
[18]T. Okubo, J. Chem. Phys. **86**, 2394 (1987).
[19]R. Kesavamoorthy, M. Rajalakshmi, and C. Babu Rao, J. Phys. Condensed Matter **1**, 7149 (1989).
[20]D. W. Schaefer and B. J. Ackerson, Phys. Rev. Lett. **35**, 1448 (1975).
[21]T. V. Ramakrishnan and M. Yussouff, Phys. Rev. B **19**, 2775 (1979).
[22]P. Salgi and Rajagopalan, Langmuir **7**, 1383 (1991).
[23]F. A. Lindemann, Z. Phys. **11**, 609 (1910).
[24]R. O. Rosenberg and D. Thirumalai, Phys. Rev. A **36**, 5690 (1987).
[25]A. J. Greenfield, J. Wellendorg, and N. M. Wiser, Phys. Rev. A **4**, 1607 (1971).
[26]J. L. Yarnell, M. J. Katz, R. G. Wenzel, and S. H. Koenig, Phys. Rev. A **7**, 2130 (1972).
[27]J. R. D. Copley and J. M. Rowe, Phys. Rev. A **9**, 1656 (1974).
[28]D. M. North, J. E. Enderly, and P. A. Egelstaff, J. Phys. C Solid State Phys. **1**, 784 (1968).
[29]L. Verlet, Phys. Rev. **165**, 201 (1968).
[30]B. J. Alder and T. E. Wainwright, J. Chem. Phys. **33**, 1439 (1960).
[31]J. P. Hansen and L. Verlet, Phys. Rev. **184**, 150 (1969).
[32]H. R. Wendt and F. F. Abraham, Phys. Rev. Lett. **41**, 1244 (1978).
[33]M. Kimura and F. Yonezawa, in *Topological Disorder in Condensed Matter*, edited by F. Yonezawa and T. Ninamiya (Springer-Verlag, Berlin, 1983).
[34]K. Binder, in *Monte Carlo Methods in Statistical Physics*, edited by K. Binder (Springer-Verlag, New York, 1979).
[35]J. P. Hansen and I. R. McDonald, *Theory of Simple Liquids* (Academic, London, 1986).
[36]R. Kesavamoorthy (private communication).
[37]P.A. Rundquist, R. Kesavamoorthy, and S. A. Asher (private communication).
[38]B. V. R. Tata, A. K. Sood, and R. Kesavamoorthy, J. Phys. **34**, 23 (1990).
[39]A. Rahman, Phys. Rev. A **136**, 405 (1964).
[40]E. M. Lifshitz and L. P. Pitaevskii, *Statistical Physics* (Pergamon, Oxford, 1980).
[41]B. V. R. Tata and A. K. Arora, J. Phys. Condensed Matter (in press).